Ray Tracing Schwarzschild & Kerr Black Holes

Mentees: Ro'aa Alkhawaja, Ali Fazal, Henry Goldberg, Serli Holluksever, Hovhannes Nercessian **Mentor:** Jason Wong

University of California, Berkeley   Undergraduate Lab at Berkeley, Physics & Astronomy Division

Abstract

This project used Python to simulate the effects of properties of Schwarzschild and Kerr black holes, on the paths taken by null geodesics. Scaling upwards from brute-force algorithms like Euler's method of integration to Python's scipy library and solve-ivp module, we started with a general simulation of a Schwarzschild black hole. Using the Runge-Kutta 4(5) method, we implemented code that solved four ordinary differential equations, describing the coordinate paths of the geodesics, that arose from Einstein's field equations of relativity [2]. In order to validate the underlying physics of our simulation, we tested the code on the precission of Mercury's perihelion, wherein the orbit shifted due to effects captured by general relativity.

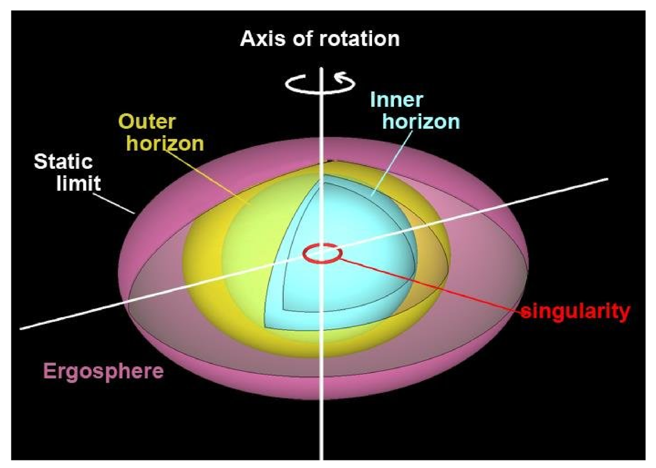

Figure 1. Black Hole Structure [1]

Background

Understanding general relativity and the motion of photons orbiting the accretion disk of black holes was key for this project. The first to do this was Viergutz, who simulated "the shape of accretion disks around Kerr black holes" in 1993 [3]. For a more general expression for black holes in space-time, Kerr metrics have been used for spinning black holes and the same metrics have been constrained for Schwarzschild black holes [4].

$$ds^2 = -(1-\frac{r_s r}{\Sigma})c^2dt^2 + \frac{\Sigma}{\Delta}dr^2 + \sum d\theta^2 + (r^2+a^2+\frac{r_s r a^2}{\Sigma}\sin^2\theta)\sin^2\theta\, d\phi^2 - \frac{2r_s r a\sin^2\theta}{\Sigma}c\,dt\,d\phi \quad (1)$$

The differential equations below are for rate-of-change quantities in the radial, theta, and phi directions (in our simulation for Schwarzschild black holes, the affine parameter q was set equal to one such that d^2t/dq^2 remained constant and equal to one) [4]. For brevity, $w = 1 - r_s/r$, where r_s is the Schwarzschild radius; and $v = 1/w$. The equations for Kerr black holes include an additional parameter a, which encodes information about the spin ($a = J/m$, or the total angular momentum per unit mass).

$$\dot{\varphi} = \frac{2ark\sin^2\theta + (r^2+a^2\cos^2\theta-2r)h}{(r^2+a^2)(r^2+a^2\cos^2\theta-2r)\sin^2\theta+2a^2rsin^4\theta} \quad (2)$$

$$\dot{\theta} = \frac{Q+(ka\cos\theta - h\cot\theta)(ka\cos\theta+h\cot\theta)}{\rho^4} \quad (3)$$

$$\dot{r} = \frac{\Delta}{\rho^2}[k\dot{t} - h\dot{\varphi} - \rho^2\dot{\theta}^2] \quad (4)$$

Runge-Kutta 4 Method

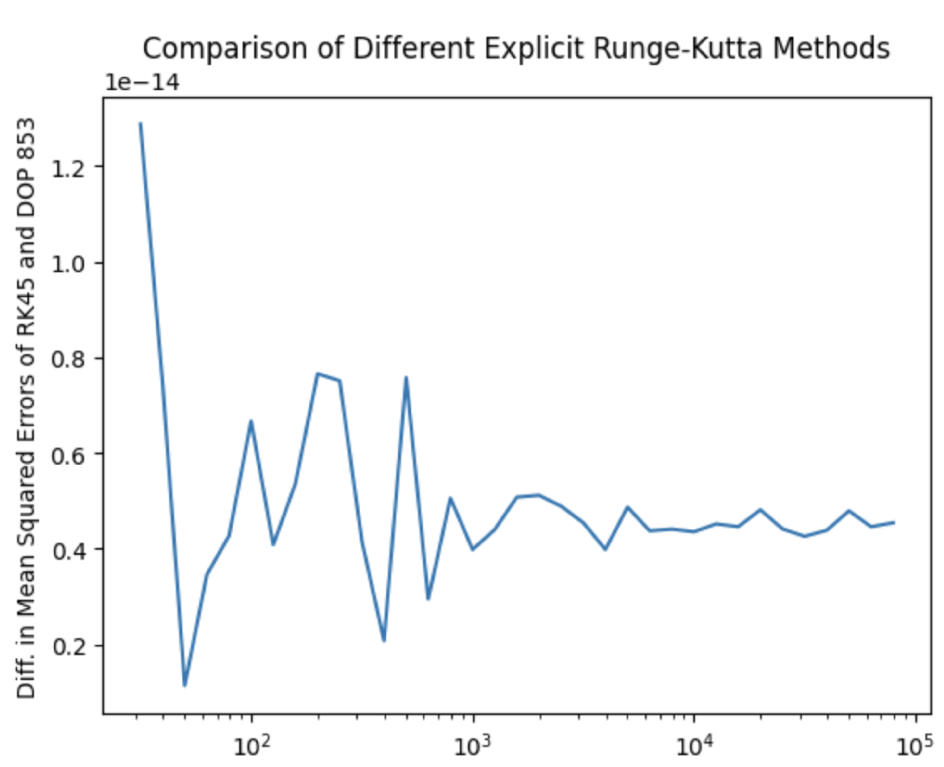

The Runge-Kutta 4(5) Method is widely regarded as the most accurate numerical method of integration. It is an algorithm that expands on the classic fourth-order method, and implements an error estimator of order five. For a first-order ODE, each subsequent value for the underlying function is determined by the present value in addition to a term characterized by: the product of a) the step size, and b) a slope estimated by a function on the right-hand side of the differential equation in question [5]. The higher-order nature of the family of Runge-Kutta methods compared to Euler's method to yield less error makes the former an ideal choice.

Schwarzschild and Kerr Simulations

The figure below showcases a stationary black hole with Schwarzschild geodesics programmed into Python. We set six different variables as our state with respect to time (r, theta, phi, and their respective derivatives), and then simulated our values using three geodesics equations with respect to the derivatives of r, theta, and phi. As we initially used spherical coordinates in the geodesic equations, we converted them to Cartesian coordinates. Additionally, the initial states were scaled via dividing by an un-normalized speed given by

$$\sqrt{\dot{r}^2+\dot{\theta}^2+\dot{\phi}^2\sin^2\theta}$$

We then graphed the equations with sample values for each state using the built-in Solve-IVP function.

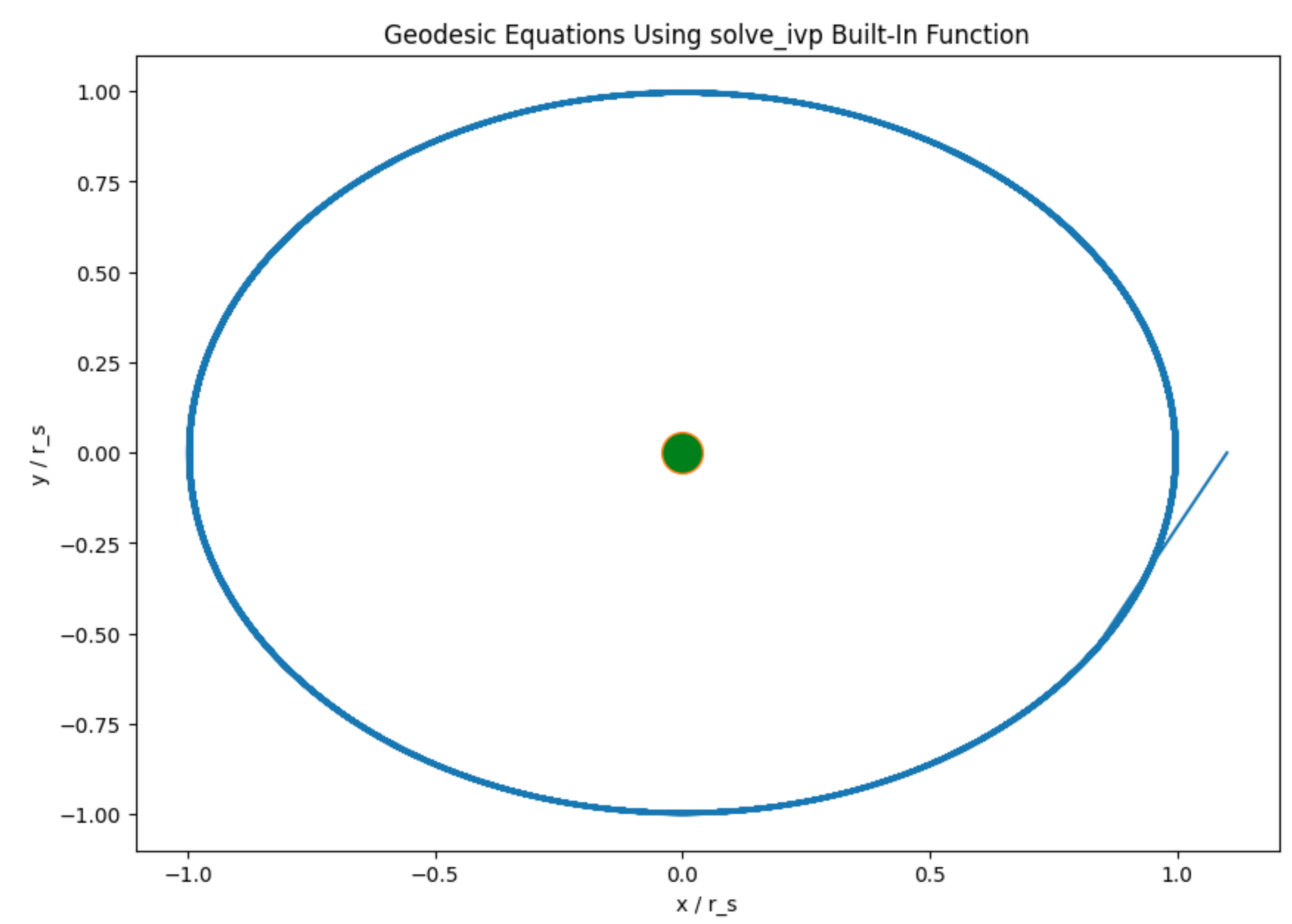

Figure 2. Position graph for a photon under the influence of a Schwarzschild black hole. Time steps of $\Delta t = 5$ seconds were used.

For spinning, Kerr black holes (below Figure), we used the same method, but using r, θ, and ϕ as our states. In addition to those states, we also had to define a multitude of other constants such as Carter's constant, as well as constants of motion including energy and angular momentum, which resulted from our choice in quantities for the initial state of the particle. It was also crucial to use a different set of 3 main geodesics equations to map our particle. After implementing the required constants and different geodesics equations, we graphed the path of a particle using Solve-IVP as well.

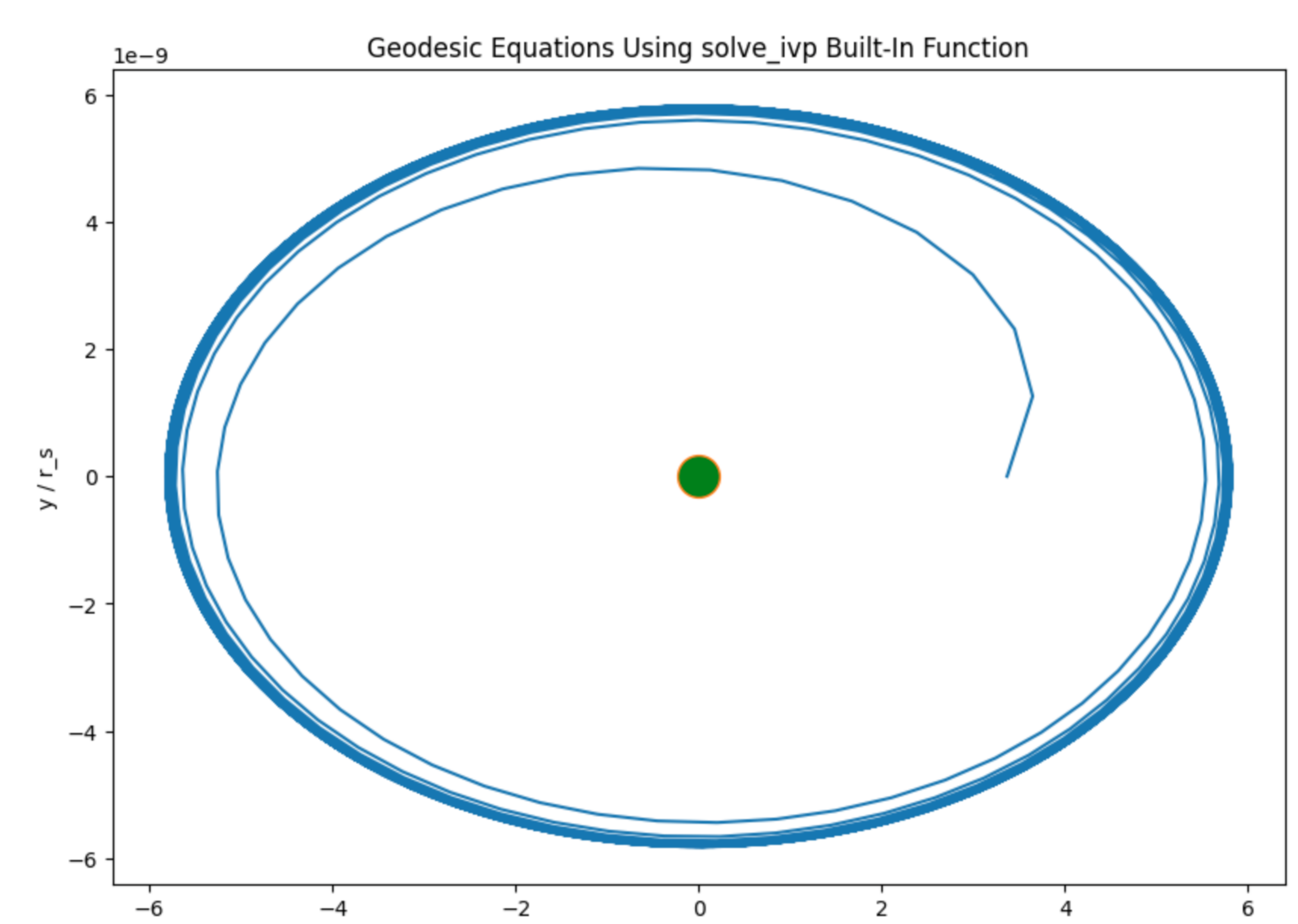

Figure 3. Position graph for a photon orbiting a Kerr black hole. Time steps of $\Delta t = 0.5$ seconds were used.

Mercury Perihelion

To validate the intuition behind the simulation, the program on Mercury's perihelion effect predicted by general relativity has been tested. Due to gravitational forces from other planets, the major axis of Mercury's orbit rotates about the Sun, causing a shift in the line that connects the Sun to the perihelion of the orbit. Einstein, through his theory of general relativity, called the precise prediction of perihelion shift the most critical test of his theory.

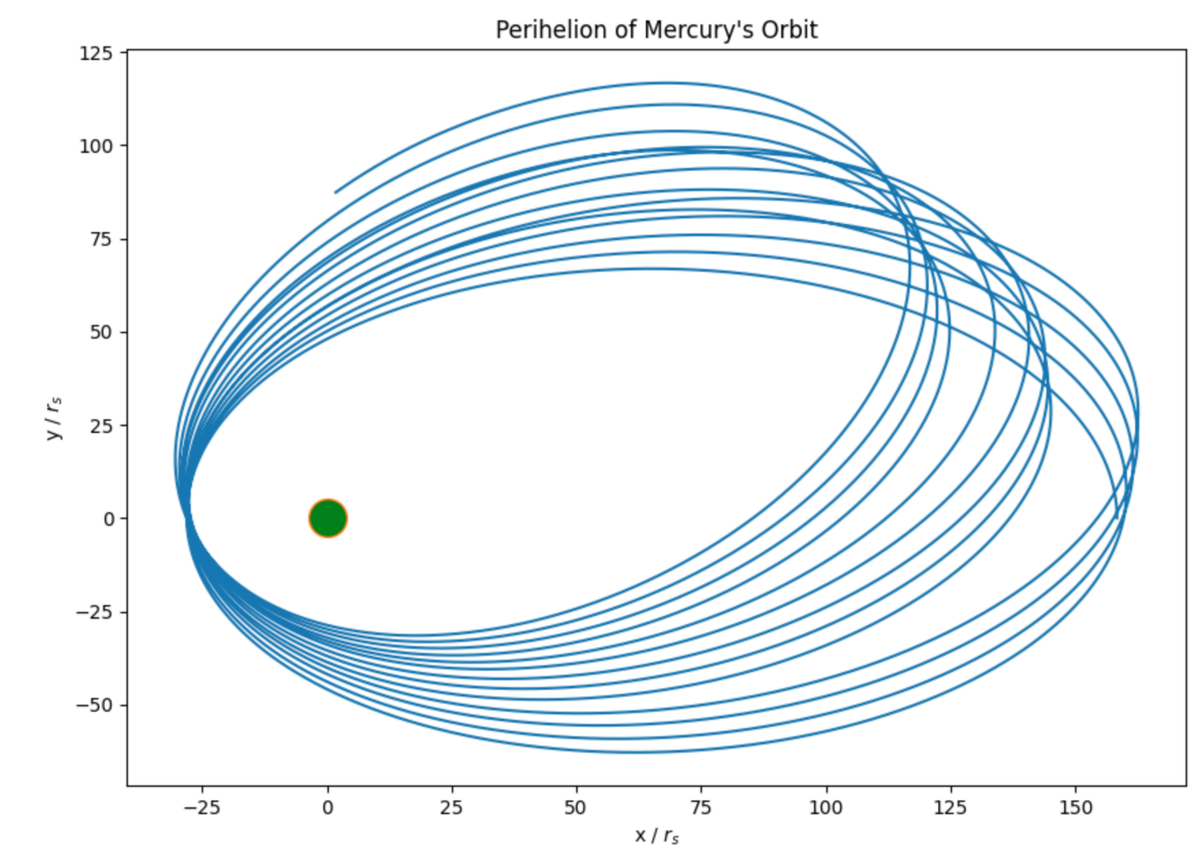

Figure 4. Shifts on Perihelion of Mercury

Future Work

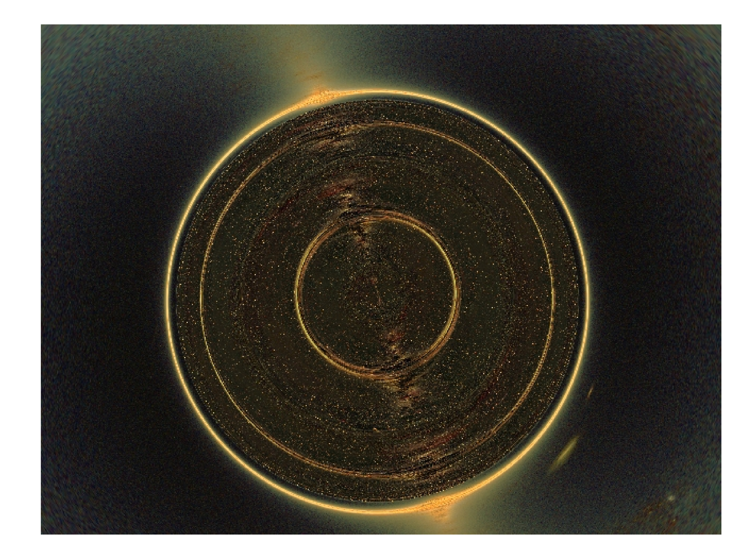

Figure 5. Reissner-Nordstrom Black Hole [6]

In the future, this project could be extended to Reissner-Nordstrom black holes and Kerr-Newman black holes, two types of charged black holes without and with spin, respectively. Thus, the simulations would include all of the types of black holes that were found by solving Einstein's equations of general relativity. Encoding models for the Kerr-Newman black hole would result in a generalization of all possible black hole types. With specific regards to the simulation, further actions could be undertaken with regards to parallelizing the code to make it more efficient among multiple CPU processors. Rendering our simulations and comparing the finished product to images made possible by the Event Horizon Telescope on the M87 supermassive black hole is also a possible step in further validation.

References

[1] K. W. GAMALATH and H. Pasan, *Structure of a rotating black hole.*

[2] C. F. Paganini, B. Ruba, and M. A. Oancea, "Characterization of null geodesics on kerr spacetimes," *arXiv preprint arXiv:1611.06927*, 2016.

[3] S. Viergutz, "Image generation in kerr geometry. i. analytical investigations on the stationary emitter-observer problem," *Astronomy and Astrophysics, Vol. 272, p. 355 (1993)*, vol. 272, p. 355, 1993.

[4] D. Wilkins and A. Fabian, "Understanding x-ray reflection emissivity profiles in agn: locating the x-ray source," *Monthly Notices of the Royal Astronomical Society*, vol. 424, no. 2, pp. 1284–1296, 2012.

[5] Z. Anastassi and T. Simos, "An optimized runge–kutta method for the solution of orbital problems," *Journal of Computational and Applied Mathematics*, vol. 175, no. 1, pp. 1–9, 2005.

[6] A. Hamilton, *Journey into and through a Reissner-Nordström black hole.*

[7] Z. Gelles, B. Prather, D. Palumbo, M. Johnson, G. Wong, and B. Georgiev, "The role of adaptive ray tracing in analyzing black hole structure," *The Astrophysical Journal*, vol. 912, no. 1, p. 39, 2021.

Acknowledgements

We would like to thank ULAB directors Rav Kaur and Anmol Desai, as well as Lab Manager Saahit Mogan and faculty advisor Dan Kasen, for their support throughout the academic year in providing necessary resources for conducting this project. Additionally, we would like to acknowledge the Discover Grant and PI Professor Eugene Chiang who made this contribution possible. Finally, we want top extend a huge thanks to everyone who attended the ULAB Physics and Astronomy division poster session and showed their support.